miR-29b is Involved in Cartilage Autophagy and Muscle Atrophy in a Rat Model of Knee Osteoarthritis

Che Ji
Huadong Hospital Affiliated to Fudan University
Jia Peiyu
Huadong Hospital Affiliated to Fudan University
Ma Yantao
Huadong Hospital Affiliated to Fudan University
Han Qi
Huadong Hospital Affiliated to Fudan University
Wang Xiaolei
Huadong Hospital Affiliated to Fudan University
Ning Xiujuan
Huadong Hospital Affiliated to Fudan University
Zheng Yongjun (zhengyongjun@fudan.edu.cn)
FuDan University

Research article

Keywords: knee osteoarthritis, microRNA, miR-29b, rat model

Posted Date: October 22nd, 2020

DOI: https://doi.org/10.21203/rs.3.rs-63574/v1

Abstract

Background

Knee osteoarthritis (KOA) is a progressively degenerative form of arthritis characterized by chondrocyte apoptosis and cartilage degeneration. KOA also involves limb muscle atrophy, especially in the quadriceps muscles. However, there are limited options for the treatment of KOA. miR-29b stimulates apoptosis in the chondrocytes from patients with KOA and muscle atrophy in other models. Therefore, we investigated the therapeutic effect of miR-29b in cartilage autophagy and muscle atrophy.

Methods

Ten rats comprised the control cohort without anterior cruciate ligament transection. The treatment group (KOA induced in the right knee via anterior cruciate ligament transection) was divided into a model untreated group and a miR-29b-antagomir group (miR-29b antagomir injected 1 wk before surgery).

Results

Real-time polymerase chain reaction revealed successful downregulation of miR-29b using antagomir in the joints and muscles. A weight-bearing test showed that miR-29b downregulation affected joint function. Enzyme-linked immunosorbent assays demonstrated that downregulating miR-29b reduced pro-inflammatory cytokine expression. Immunohistochemistry revealed that miR-29b depletion enhanced autophagy by activating LC3 and beclin-1 in the cartilage. Autophagy was stimulated by the activation of MAPK and mTOR signaling. Depletion of miR-29b ameliorated the decrease in the weight of the quadriceps and the quadriceps weight/body weight ratio of the rats. Hematoxylin–eosin and periodic acid–Schiff staining showed that miR-29b downregulation inhibited muscular atrophy. Immunofluorescence showed that miR-29b downregulation affected IGF/PI3K/AKT signaling.

Conclusions

This study demonstrated the therapeutic effect of miR-29b on autophagy in the cartilage and on muscle atrophy in a rat model for KOA, highlighting the potential of miR-29b as a therapeutic target for KOA.

1. Background

Osteoarthritis (OA) affects the global population that is more than 45 years of age, especially those over 65 years [1]. OA markedly reduces the quality of life and is an economic burden to patients and their families [2]. Among all the joints in the body, OA commonly affects the knees and hips. Trauma and degeneration in the joints, such as anterior cruciate ligament tears and cartilage degeneration, primarily result in knee osteoarthritis (KOA) [3]. The pathogenesis of KOA involves inflammation, cartilage

destruction, and subchondral bone sclerosis [4]. KOA is characterized by knee pain and the inability to move, stand, and bend. Another symptom associated with KOA is muscle atrophy in the lower limbs, especially in the quadriceps [5, 6]. This increases risks associated with walking, difficulty in standing or getting up, and falling. Limb muscle atrophy plays a crucial role in the pathogenesis of KOA [7]. Therefore, alleviation of muscle atrophy and weakness may help prevent and/or treat KOA [8].

MicroRNAs are single-stranded non-coding RNAs that inhibit translation or induce target mRNA degradation. Studies have shown the involvement of microRNAs in muscle activity, such as miR-29 [9], miR-149-5p [9], miR-155 [11], miR-206 [12], and miR-491 [13]. The miR-29 family comprises three members: miR-29a, miR-29b, and miR-29c. The miR-29 family plays multiple roles in muscle development [14]. miR-29b is involved in different mechanisms of muscle atrophy, including aging, cancer, and fasting, by targeting PI3K/AKT signaling [15]. The downregulation of miR-29b causes muscle atrophy and leads to chronic kidney disease [16, 17]. Unlike the prevalent clarity on bone and cartilage pathology, the intrinsic mechanism and progression involved in muscle atrophy of patients with KOA remain to be elucidated. Studies have indicated that muscle atrophy in KOA involves arthrogenic muscle inhibition, which is induced by abnormalities in the knee joint but not by aging, cancer, toxicity, and fasting [18]. Therefore, the role of miR-29b in muscle atrophy in patients with KOA needs to be investigated.

Chondrocyte cell death is an important aspect of KOA pathogenesis. Type 1 and 2 cell death include apoptosis and autophagy, respectively. The past decades have focused on apoptosis in chondrocytes for the treatment of KOA. Recent studies have suggested that autophagy is also important and can help prevent KOA and alleviate its symptoms [19, 20]. miR-29b-3p is overexpressed in patients with KOA [21], and upon inhibition, apoptosis is ameliorated in KOA by targeting progranulin [22]. However, the effect of miR-29b on autophagy in chondrocytes remains to be explored.

The aim of this study was to elucidate the therapeutic role of miR-29b and its mechanisms involved in muscle atrophy in individuals with KOA. Moreover, we investigated the role of miR-29b in chondrocyte autophagy.

2. Methods

2.1 Chemicals and agents

The kits for protein extraction, BCA protein estimation, and periodic acid–Schiff (PAS) staining were purchased from Beyotime Institute of Biotechnology (Haimeng, China). TRIzol was procured from Sigma-Aldrich (St. Louis, MO, USA). The antagomir against miR-29b was designed and synthesized by Gene Pharma (Shanghai, China). Enzyme-linked immunosorbent assays were obtained from R&D Systems (Minneapolis, MN, USA). Primary antibodies and secondary antibodies were purchased from Abcam (Cambridge, UK). All other chemicals were of analytical grade.

2.2 Animals and treatment

All animal experiments were approved by the Institutional Animal Care and Use Committee of Fudan University (approval number 202006007S). Female Sprague–Dawley (SD) rats [150–160 g, 6-wk-old, healthy, and specific-pathogen free (SPF)] were obtained from Shanghai SIPPR-Bk Lab Animal Co., Ltd., and housed at Fudan University in an SPF environment with a temperature of 20–25 °C, humidity of 40% ± 5%, and 12 h light/dark cycles. Rats were maintained in a cage with sawdust bedding and free access to adequate diet-maintaining pellets for rats/mice and SPF-grade water.

A total of 30 SD rats were distributed into three groups: 10 rats comprised the control cohort without anterior cruciate ligament transection (ACLT), and 20 rats constituted the OA group with ACLT. After ACLT, the 20 rats were further divided into two groups of 10 rats each: a model group (receiving no treatment) and miR-29b-antagomir group (receiving miR-29b antagomir 1 wk before ACLT). The animal experiment lasted for 5 wk. At the end of the experiment, the anesthetized rats were euthanized by CO2 in an animal-euthanasia chamber (45 × 30 × 30 cm), and the fill rate of carbon dioxide was 100% with the gas flow rate kept at 45L/min.

2.3 Anesthetic method and surgery

ACLT was performed as previously described [20] under anesthesia using pentobarbital sodium at 40 mg/kg (intraperitoneal) and a maintenance mixture of O_2 and isoflurane (2.5%). After the anterior cruciate ligament was transected, rats were subjected to the drawer test to ensure successful operation. Subsequently, the rats were permitted free activity in the cage and injected with penicillin (Beyotime, Haimeng, China) to avoid infection.

2.4 Behavior study

A weight-bearing distribution test was performed as described previously [20]. Briefly, a dual-channel weight average was used to measure the weight distribution of the hind paws every week. The index of joint discomfort and function was calculated as the ratio of the experimental right sides to the untreated left sides.

2.5 Muscle weight and morphology

After the administration of antagomir, we recorded the body weight (BW), quadriceps muscle weight (QW), and quadriceps muscle weight/body weight (QW/BW) ratio. Subsequently, we analyzed the morphology of the quadriceps muscle. Briefly, the quadriceps muscle samples were washed using phosphate-buffered saline, fixed in formaldehyde, and embedded in paraffin as described previously[23]. The muscles were cut into 5-μm-thick sections and stained using hematoxylin–eosin (HE). The staining profile was visualized using light microscopy (MF31; Mshot, Guangzhou, China). The myofiber cross-sectional area and diameter were calculated as per previous reports [24, 25]. For PAS staining, the sections were incubated in 0.5% periodate solution and stained using the PAS staining kit following the protocol provided.

2.6 Joint morphology and ankle histological scores

After the last injection, knee joint morphology was assayed per a previously published report [26]. The right knee joints of rats were harvested, fixed using 10% paraformaldehyde, embedded, and sectioned into 5 μm slices. The sections were subjected to HE staining and toluidine blue, followed by visualization using light microscopy. Arthritic histology was analyzed using Mankin scores by a third-party pathologist [27, 28].

2.7 Serum cytokines

Briefly, rat blood was harvested and centrifuged at 4,000 rpm/min for 10 min, and the supernatants were collected into tubes. The concentrations of tumor necrosis factor-α (TNF-α) and interleukin-1β (IL-1β) in rat sera were quantified using enzyme-linked immunosorbent assays following the kit protocol.

2.8 Immunohistochemistry (IHC)

IHC was performed to detect autophagy in the rat knee joints [29]. The joints were harvested and fixed. After 2 months of mild decalcification, samples were cut into 5-μm sections. The sections were incubated overnight at 4 °C with rabbit polyclonal antibody against specific proteins (p-ERK, Abcam, No: ab192591, 1:100; p-P38, Abcam, No: 170099, 1:100; mTOR: Abcam, No: ab109268, 1:100; LC3B: Abcam, No: 48394, 1:100; and Beclin-1: Abcam, No: 210498, 1:100). The sections were washed and incubated with an anti-rabbit horseradish peroxidase-conjugated secondary antibody for 10 min at room temperature and visualized by light microscopy.

2.9 Immunofluorescence

Immunofluorescence was performed to assay the quadriceps from the three groups. Samples were collected, fixed with 4% pre-cooled paraformaldehyde, and embedded in paraffin. Subsequently, the muscles were cut into 5-μm sections and incubated with primary antibodies (PI3K: Abcam, No: 140307, 1:100; p-AKT: Abcam, No: 38449, 1:100). Images were captured using a slide-driver fluorescence microscope (3DHistech Ltd., Budapest, Hungary) to analyze the intensity of staining. The images were processed using Image-Pro Plus software 6.0.

2.10 RNA isolation, cDNA synthesis, and real-time polymerase chain reaction (qPCR)

RNA was isolated using TRIzol (Takara), and cDNA was synthesized using the Mir-X™ miRNA FirstStrand Synthesis system (Takara) using the protocol provided. Each qPCR volume (20 μL) was set up using 50 ng of cDNA, 200 μM of the desired primer, and TB Green® qRT-PCR (1×) and analyzed using 40 cycles of 5 s at 95 °C, 20 s at 60 °C, and 10 s at 95 °C using the Applied Biosystems® StepOne RT-PCR system. The housekeeping gene *U6* was used as the internal standard for qPCR using the following primers: forward, 5'-GGAACGATACAGAGAAGATTAGC-3' and reverse, 5'-TGGAACGCTTCACGAATTTGC-G-3'. The primers used to amplify miR-29a, miR-29b, and miR-29c were 5'-CGCTAGCACCATCTGAAATCGGTTA-3', 5'-CGCGTAGCACCATTTGAAATCAGTGTT-3', and 5'-CGCGTAGCACCATTTGAAATCGGTTA-3'.

2.11 Statistical analysis

Data are represented as mean ± standard deviation and were analyzed using one-way analysis of variance followed by the Bonferroni test. $P < 0.05$ was considered statistically significant. All statistical analyses were performed using SPSS22.0 (Chicago, IL, USA) and plotted using GraphPad Prism 6.0 (San Diego, CA, USA). The person who did the data analysis did not have any information regarding the research design and methods.

3. Results

3.1 Functional and histological changes of the knee joint in the KOA model

The right hind limb of all the SD rats bore ~ 50% of the weight 1 wk before ACLT, suggesting a balance between left and right knee function (Fig. 1A). Rats treated with/without antagomir against miR-29b showed a reduction in the ability of the right hind limb to bear weight after ACLT. The miR-29b antagomir ameliorated the extent of this decrease, indicating the involvement of miR-29b in the recovery of the right knee. HE staining revealed histological changes, such as synovial proliferation, inflammatory infiltrates, angiogenesis, edema, pannus formation, granuloma, focal loss of cartilage, bone erosion, and presence of extra-articular inflammation in the model group. Downregulation of miR-29b alleviated these phenotypes (Fig. 1B). Mankin scores were higher in the model group than in the control group. However, Mankin scores decreased in the antagomir group as compared to those in the model group (Fig. 1C). Furthermore, Masson and toluidine blue staining showed differences in the structural alterations in the cartilages. The thicknesses of cartilage in the model group were lower than those in the control group, while downregulating miR-29b enhanced cartilage thickness (Fig. 1D and 1E), indicating that downregulating miR-29b alleviates the symptoms of KOA.

3.2 Histological changes in the limb muscle of rats with KOA

We successfully confirmed muscle atrophy (Fig. 2A) in the model group as compared to the control group. Depleting rats of miR-29b alleviated the atrophy in the quadriceps muscles. Muscle atrophy was evaluated based on the decrease in QW, ratio of QW/BW, grip strength, myotube cross-sectional area and diameter (HE staining), and mitochondria and glycogen content (PAS staining). Figure 2B shows the decrease in QW and QW/BW in the model group. The downregulation of miR-29b ameliorated the decrease in QW and QW/BW ratio. Moreover, the downregulation of miR-29b increased muscle fiber cross-sectional area, diameter of quadriceps, diameter of muscle fiber (Fig. 2C and 2D), and mitochondrial and glycogen content in the quadriceps (Fig. 2E).

3.3 TNF-α and IL-1β levels in the sera of SD rats with KOA

We observed a marked increase in the levels of pro-inflammatory cytokines in the serum of SD rats in the model group compared to those in the control group. Depleting miR-29b rescued this increase (Fig. 3A and 3B). TNF-α levels in the model group were high, while those in the antagomir group were low. We detected a similar trend for IL-1β levels in the sera from these rats.

3.4 Autophagy in the cartilage and atrophy-associated signaling

qPCR confirmed the downregulation of miR-29b in the antagomir group, with no off-target effects on miR-29a and miR-29c expression in the muscles and joints (Fig. 4A–4F). miR-29b expression increased in the joints and muscles of rats in the KOA model group; this was in accordance with the findings of Chen et al. [22] and Chan et al. [15], respectively. Autophagy-related proteins, such as beclin-1 and LC3, were upregulated by the depletion of miR-29b (Fig. 5A and 5B). Moreover, IHC demonstrated that depleting miR-29b downregulated p-ERK and p-38 in the cartilage as compared to that in the cartilage of rats in the KOA model group (Fig. 5C and 5D). mTOR levels reduced with the downregulation of miR-29b as compared to mTOR levels in the model group (Fig. 5E). Immunofluorescence showed that downregulating miR-29b reduced the expression of the atrophy-related proteins PI3K and p-AKT in the quadriceps (Fig. 6–8).

4. Discussion

KOA is a debilitating disease that leads to knee dysfunction, disability, and poor quality of life in patients. The underlying mechanisms of KOA pathogenesis involve apoptosis in the chondrocytes, inflammation, and reduced autophagy. Autophagy is essential for normal cellular function. Apoptosis is crucial for normal cellular activity and recycling of organellar material during nutrient deficiency or stress-related inflammation, ischemia, or excessive production of reactive oxygen species. Studies have shown that autophagy in chondrocytes is important for the development of KOA. Recent reports have also linked autophagy to inflammation. Inflammation inhibits autophagy and promotes disease in the knee joint in individuals with KOA [30]. Thus, regulated autophagy might be a novel therapeutic strategy for KOA. Agents such as *Butea monosperma* flower extract and ozone have been found to reduce the levels of pro-inflammatory cytokines in *in vitro*-regulated autophagy models [30, 31]. Exercise using the treadmill has also been found to activate autophagy (via multiple signaling pathways) and ameliorate the symptoms associated with KOA in rats [32]. Increases in LC3B and beclin-1 in models with KOA stimulate autophagy in chondrocytes [32]. In this study, miR-29b enhanced the levels of the autophagy-related proteins LC3B and beclin-1, which alleviated the symptoms associated with KOA.

The MAPK signaling pathway comprises P38, ERK, and JNK and is involved in KOA pathogenesis *in vitro* [33, 34] and *in vivo* [35, 36]. MAPK signaling is an important mediator of synovial inflammation. NF-κB signaling modulates apoptosis in chondrocytes, which is essential for nitric oxide-induced apoptosis in articular chondrocytes [37] and leads to the activation of P38 [38]. mTOR is a signaling pathway that is involved in cell growth and differentiation and is downstream of the AKT and MAPK signaling pathways.

mTOR signaling inhibits cellular catabolism by blocking autophagy in KOA models. Therefore, mTOR might be an efficient therapeutic target for KOA. Rapamycin inhibits mTOR signaling and activates autophagy, thereby restoring the synthesis of catabolic enzymes and alleviating the symptoms of KOA in mice [39]. In this study, we investigated the importance of MAPK signaling in a rat model depleted of miR-29b.

KOA affects muscle function around the joints [40]. The muscles around the knees are important for joint movement and maintaining joint stability. These muscles also protect the knees from stress and improve proprioception. Therefore, muscle damage may affect the occurrence, development, and severity of arthritis. Moreover, since arthritis has a negative impact on muscle function, it further augments disease progression and forms a vicious cycle of joint degradation, muscle weakness, and muscle atrophy [41, 42]. The cross-sectional area of muscles in the lower extremities are lowered by 12–19% in patients with hip or knee arthritis[43, 44]. Muscle atrophy occurs when protein degradation exceeds synthesis and is induced in adult skeletal muscle in a variety of conditions, including starvation, denervation, cancer cachexia, heart failure, and aging [45]. The primary molecular mechanisms underlying muscle atrophy involve reduced protein synthesis, increased proteolysis, and impaired regeneration of muscle satellite cells [46]. IGF-1/AKT signaling is associated with protein synthesis. We found elevated levels of miR-29b and reduced IGF-1/AKT signaling in the muscles of rats with KOA. Downregulating miR-29b enhanced IGF-1/AKT signaling, upregulated protein synthesis, and stimulated anti-atrophy. Pro-inflammatory cytokines such as TNF-α and IL-1β are associated with articular cartilage disease and enhanced catabolism in inflammatory diseases. These cytokines also trigger muscle atrophy [47, 48]. miR-29b downregulated the levels of these pro-inflammatory cytokines.

Conclusion

To sum up, this study revealed an ameliorative effect of miR-29b on autophagy in the cartilage and muscle atrophy in a rat model in KOA. Depleting rats of miR-29b promoted limb function recovery and alleviated cartilage damage and the atrophy in the quadriceps muscles. MAPK signaling in the cartilage and PI3K/AKT signaling in the muscle play important roles in the therapeutic effect of miR-29b. Thus, miR-29b may serve as a therapeutic target for KOA.

Abbreviations

OA: Osteoarthritis; KOA: Knee osteoarthritis; ACLT: Anterior cruciate ligament transection; TNF-α: Tumor necrosis factor alpha; IL-1β: Interleukin-1β; MAPK: Mitogen-activated protein kinase; mTOR: Mammalian target of rapamycin; HE: Hematoxylin–eosin; PAS: Periodic acid–Schiff; IGF: Insulin-like growth factor 1; PI3K: Phosphatidylinositol 3-kinase; AKT: Protein kinase B; BW: Body weight; QW: Quadriceps weight; IHC: Immunohistochemistry; miRNAs: MicroRNAs; qPCR: Real-time polymerase chain reaction; SPF: Specific-pathogen free

Declarations

Ethics approval and consent to participate

This study was approved by the Ethical Committee of Fudan University, China.

Consent for publication

Not applicable.

Availability of data and materials

The datasets used and/or analysed during the current study are available from the corresponding author on reasonable request.

Competing interest

The authors declare that they have no competing interests.

Funding Details

This work was supported by the Shanghai Key disciplines program of Health and Family Planning [Grant No: 2017ZZ02010].

Authors' contributions

Contributions: (I) Conception and design: J Che, P Jia, Y Zheng; (II) Administrative support: Y Zheng; (III) Provision of study materials or patients: Y Ma, Q Han, X Wang, X Ning; (IV) Collection and assembly of data: J Che, J Jia, X Ning; (V) Data analysis and interpretation: J Che, P Jia; (VI) Manuscript writing: All authors; (VII) Final approval of manuscript: All authors.

Acknowledgements

Not applicable.

References

1. Liu Y, Zhang H, Liang N, Fan W, Li J, Huang Z, Yin Z, Wu Z, Hu J. Prevalence and associated factors of knee osteoarthritis in a rural Chinese adult population: an epidemiological survey. BMC PUBLIC HEALTH. 2016;16:94.

2. Carmona-Teres V, Moix-Queralto J, Pujol-Ribera E, Lumillo-Gutierrez I, Mas X, Batlle-Gualda E, Gobbo-Montoya M, Jodar-Fernandez L, Berenguera A. Understanding knee osteoarthritis from the patients' perspective: a qualitative study. BMC Musculoskelet Disord. 2017;18(1):225.
3. Dulay GS, Cooper C, Dennison EM. Knee pain, knee injury, knee osteoarthritis & work. Best Pract Res Clin Rheumatol. 2015;29(3):454–61.
4. Muratovic D, Findlay DM, Cicuttini FM, Wluka AE, Lee YR, Kuliwaba JS. Bone matrix microdamage and vascular changes characterize bone marrow lesions in the subchondral bone of knee osteoarthritis. BONE. 2018;108:193–201.
5. Kus G, Yeldan I. Strengthening the quadriceps femoris muscle versus other knee training programs for the treatment of knee osteoarthritis. RHEUMATOL INT. 2019;39(2):203–18.
6. Noehren B, Kosmac K, Walton RG, Murach KA, Lyles MF, Loeser RF, Peterson CA, Messier SP. Alterations in quadriceps muscle cellular and molecular properties in adults with moderate knee osteoarthritis. Osteoarthritis Cartilage. 2018;26(10):1359–68.
7. Ikeda S, Tsumura H, Torisu T. Age-related quadriceps-dominant muscle atrophy and incident radiographic knee osteoarthritis. J ORTHOP SCI. 2005;10(2):121–6.
8. Hussain SM, Neilly DW, Baliga S, Patil S, Meek R. Knee osteoarthritis: a review of management options. Scott Med J. 2016;61(1):7–16.
9. Wang K, Yu J, Wang B, Wang H, Shi Z, Li G. miR-29a Regulates the Proliferation and Migration of Human Arterial Smooth Muscle Cells in Arteriosclerosis Obliterans of the Lower Extremities. Kidney Blood Press Res. 2019;44(5):1219–32.
10. Zhang B, Dong Y, Liu M, Yang L, Zhao Z. miR-149-5p Inhibits Vascular Smooth Muscle Cells Proliferation, Invasion, and Migration by Targeting Histone Deacetylase 4 (HDAC4). Med Sci Monit. 2019;25:7581–90.
11. Artlett CM, Sassi-Gaha S, Hope JL, Feghali-Bostwick CA, Katsikis PD. Mir-155 is overexpressed in systemic sclerosis fibroblasts and is required for NLRP3 inflammasome-mediated collagen synthesis during fibrosis. ARTHRITIS RES THER. 2017;19(1):144.
12. Matsuzaka Y, Tanihata J, Komaki H, Ishiyama A, Oya Y, Ruegg U, Takeda SI, Hashido K. Characterization and Functional Analysis of Extracellular Vesicles and Muscle-Abundant miRNAs (miR-1, miR-133a, and miR-206) in C2C12 Myocytes and mdx Mice. PLOS ONE. 2016;11(12):e167811.
13. He J, Wang F, Zhang P, Li W, Wang J, Li J, Liu H, Chen X. miR-491 inhibits skeletal muscle differentiation through targeting myomaker. ARCH BIOCHEM BIOPHYS. 2017;625–626:30–8.
14. O'Reilly S. MicroRNAs in fibrosis: opportunities and challenges. ARTHRITIS RES THER. 2016;18:11.
15. Li J, Chan MC, Yu Y, Bei Y, Chen P, Zhou Q, Cheng L, Chen L, Ziegler O, Rowe GC, et al. miR-29b contributes to multiple types of muscle atrophy. NAT COMMUN. 2017;8:15201.
16. Wang XH, Hu Z, Klein JD, Zhang L, Fang F, Mitch WE. Decreased miR-29 suppresses myogenesis in CKD. J AM SOC NEPHROL. 2011;22(11):2068–76.

17. Wang H, Wang B, Zhang A, Hassounah F, Seow Y, Wood M, Ma F, Klein JD, Price SR, Wang XH. Exosome-Mediated miR-29 Transfer Reduces Muscle Atrophy and Kidney Fibrosis in Mice. MOL THER. 2019;27(3):571–83.
18. Cunha JE, Barbosa GM, Castro P, Luiz B, Silva A, Russo TL, Vasilceac FA, Cunha TM, Cunha FQ, Salvini TF. Knee osteoarthritis induces atrophy and neuromuscular junction remodeling in the quadriceps and tibialis anterior muscles of rats. Sci Rep. 2019;9(1):6366.
19. Lian WS, Ko JY, Wu RW, Sun YC, Chen YS, Wu SL, Weng LH, Jahr H, Wang FS: **MicroRNA-128a represses chondrocyte autophagy and exacerbates knee osteoarthritis by disrupting Atg12**. *CELL DEATH DIS* 2018, **9**(9):919.
20. Chen CH, Ho ML, Chang LH, Kang L, Lin YS, Lin SY, Wu SC, Chang JK. Parathyroid hormone-(1–34) ameliorated knee osteoarthritis in rats via autophagy. J Appl Physiol (1985). 2018;124(5):1177–85.
21. Le LT, Swingler TE, Crowe N, Vincent TL, Barter MJ, Donell ST, Delany AM, Dalmay T, Young DA, Clark IM. The microRNA-29 family in cartilage homeostasis and osteoarthritis. J Mol Med (Berl). 2016;94(5):583–96.
22. Chen L, Li Q, Wang J, Jin S, Zheng H, Lin J, He F, Zhang H, Ma S, Mei J, et al. MiR-29b-3p promotes chondrocyte apoptosis and facilitates the occurrence and development of osteoarthritis by targeting PGRN. J CELL MOL MED. 2017;21(12):3347–59.
23. Sheriffs IN, Rampling D, Smith VV. Paraffin wax embedded muscle is suitable for the diagnosis of muscular dystrophy. J CLIN PATHOL. 2001;54(7):517–20.
24. GB D, SM P, TL JLD, IL B R, AS MF, TF M. S: Quadriceps muscle atrophy after anterior cruciate ligament transection involves increased mRNA levels of atrogin-1, muscle ring finger 1, and myostatin. AM J PHYS MED REHAB. 2013;92(5):411–9.
25. K T HSASKARSAH. A J, K S, Y C, M Y et al: Mechanisms of cisplatin-induced muscle atrophy. TOXICOL APPL PHARM. 2014;278(2):190–9.
26. Giunta S, Castorina A, Marzagalli R, Szychlinska MA, Pichler K, Mobasheri A, Musumeci G. Ameliorative effects of PACAP against cartilage degeneration. Morphological, immunohistochemical and biochemical evidence from in vivo and in vitro models of rat osteoarthritis. INT J MOL SCI. 2015;16(3):5922–44.
27. Jhun J, Lee SH, Na HS, Seo H, Kim E, Moon S, Jeong J, Lee DH, Kim SJ, Cho M. The chicken combs extract alleviates pain and cartilage degradation in rat model osteoarthritis. TISSUE ENG REGEN MED. 2015;12(5):352–61.
28. Mankin HJ, Dorfman H, Lippiello L, Zarins A. Biochemical and metabolic abnormalities in articular cartilage from osteo-arthritic human hips. II. Correlation of morphology with biochemical and metabolic data. J BONE JOINT SURG AM. 1971;53(3):523–37.
29. Feng FB, Qiu HY. Effects of Artesunate on chondrocyte proliferation, apoptosis and autophagy through the PI3K/AKT/mTOR signaling pathway in rat models with rheumatoid arthritis. BIOMED PHARMACOTHER. 2018;102:1209–20.

30. Zhao X, Li Y, Lin X, Wang J, Zhao X, Xie J, Sun T, Fu Z. Ozone induces autophagy in rat chondrocytes stimulated with IL-1beta through the AMPK/mTOR signaling pathway. J PAIN RES. 2018;11:3003–17.
31. Ansari MY, Khan NM, Haqqi TM. A standardized extract of Butea monosperma (Lam.) flowers suppresses the IL-1beta-induced expression of IL-6 and matrix-metalloproteases by activating autophagy in human osteoarthritis chondrocytes. BIOMED PHARMACOTHER. 2017;96:198–207.
32. Zhang X, Yang Y, Li X, Zhang H, Gang Y, Bai L. Alterations of autophagy in knee cartilage by treatment with treadmill exercise in a rat osteoarthritis model. INT J MOL MED. 2019;43(1):336–44.
33. Xu K, Ma C, Xu L, Ran J, Jiang L, He Y, Adel AMS, Wang Z, Wu L. Polygalacic acid inhibits MMPs expression and osteoarthritis via Wnt/beta-catenin and MAPK signal pathways suppression. INT IMMUNOPHARMACOL. 2018;63:246–52.
34. Li X, Guo Y, Huang S, He M, Liu Q, Chen W, Liu M, Xu D, He P. Coenzyme Q10 Prevents the Interleukin-1 Beta Induced Inflammatory Response via Inhibition of MAPK Signaling Pathways in Rat Articular Chondrocytes. Drug Dev Res. 2017;78(8):403–10.
35. Xue JF, Shi ZM, Zou J, Li XL. Inhibition of PI3K/AKT/mTOR signaling pathway promotes autophagy of articular chondrocytes and attenuates inflammatory response in rats with osteoarthritis. BIOMED PHARMACOTHER. 2017;89:1252–61.
36. Wu Z, Luan Z, Zhang X, Zou K, Ma S, Yang Z, Feng W, He M, Jiang L, Li J, et al. Chondro-protective effects of polydatin in osteoarthritis through its effect on restoring dysregulated autophagy via modulating MAPK, and PI3K/Akt signaling pathways. Sci Rep. 2019;9(1):13906.
37. Liacini A, Sylvester J, Li WQ, Huang W, Dehnade F, Ahmad M, Zafarullah M. Induction of matrix metalloproteinase-13 gene expression by TNF-alpha is mediated by MAP kinases, AP-1, and NF-kappaB transcription factors in articular chondrocytes. EXP CELL RES. 2003;288(1):208–17.
38. Roman-Blas JA, Jimenez SA. NF-kappaB as a potential therapeutic target in osteoarthritis and rheumatoid arthritis. Osteoarthritis Cartilage. 2006;14(9):839–48.
39. Carames B, Hasegawa A, Taniguchi N, Miyaki S, Blanco FJ, Lotz M. Autophagy activation by rapamycin reduces severity of experimental osteoarthritis. ANN RHEUM DIS. 2012;71(4):575–81.
40. Bennell KL, Wrigley TV, Hunt MA, Lim BW, Hinman RS. Update on the role of muscle in the genesis and management of knee osteoarthritis. Rheum Dis Clin North Am. 2013;39(1):145–76.
41. Levinger I, Levinger P, Trenerry MK, Feller JA, Bartlett JR, Bergman N, McKenna MJ, Cameron-Smith D. Increased inflammatory cytokine expression in the vastus lateralis of patients with knee osteoarthritis. Arthritis Rheum. 2011;63(5):1343–8.
42. Terracciano C, Celi M, Lecce D, Baldi J, Rastelli E, Lena E, Massa R, Tarantino U. Differential features of muscle fiber atrophy in osteoporosis and osteoarthritis. Osteoporos Int. 2013;24(3):1095–100.
43. Arokoski MH, Arokoski JP, Haara M, Kankaanpaa M, Vesterinen M, Niemitukia LH, Helminen HJ. Hip muscle strength and muscle cross sectional area in men with and without hip osteoarthritis. J RHEUMATOL. 2002;29(10):2185–95.

44. Rasch A, Bystrom AH, Dalen N, Berg HE. Reduced muscle radiological density, cross-sectional area, and strength of major hip and knee muscles in 22 patients with hip osteoarthritis. ACTA ORTHOP. 2007;78(4):505–10.
45. Schiaffino S, Dyar KA, Ciciliot S, Blaauw B, Sandri M. Mechanisms regulating skeletal muscle growth and atrophy. FEBS J. 2013;280(17):4294–314.
46. Cohen S, Nathan JA, Goldberg AL. Muscle wasting in disease: molecular mechanisms and promising therapies. NAT REV DRUG DISCOV. 2015;14(1):58–74.
47. Cheung WW, Paik KH, Mak RH. Inflammation and cachexia in chronic kidney disease. PEDIATR NEPHROL. 2010;25(4):711–24.
48. VanderVeen BN, Fix DK, Carson JA. Disrupted Skeletal Muscle Mitochondrial Dynamics, Mitophagy, and Biogenesis during Cancer Cachexia: A Role for Inflammation. OXID MED CELL LONGEV. 2017;2017:3292087.

Figures

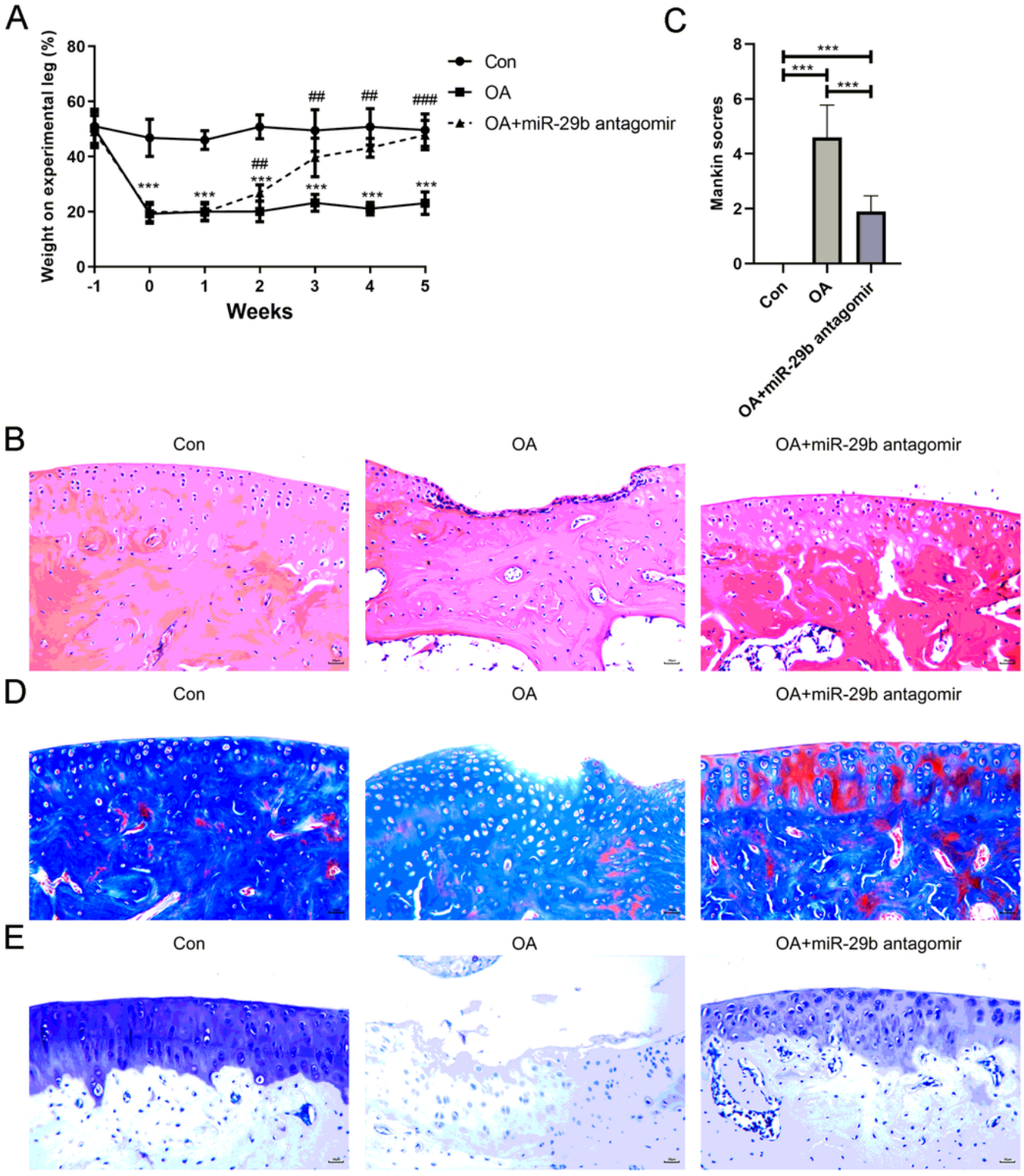

Figure 1

Behavior and morphology of the knee joint in a Sprague-Dawley rat model of knee osteoarthritis (KOA). (A) Weight-bearing assay. (B) Hematoxylin–eosin staining of the cartilage in the knee joint. (C) Mankin scores across the different groups of rats. (D) Masson staining of the cartilage in the knee joint. (E) Toluidine blue staining of the cartilage in the knee joint. Scale bar = 25 μm. *P < 0.05, **P < 0.01, and ***P < 0.001 (model group); ##P < 0.01 and ###P < 0.001 (other groups; comparison with the KOA group).

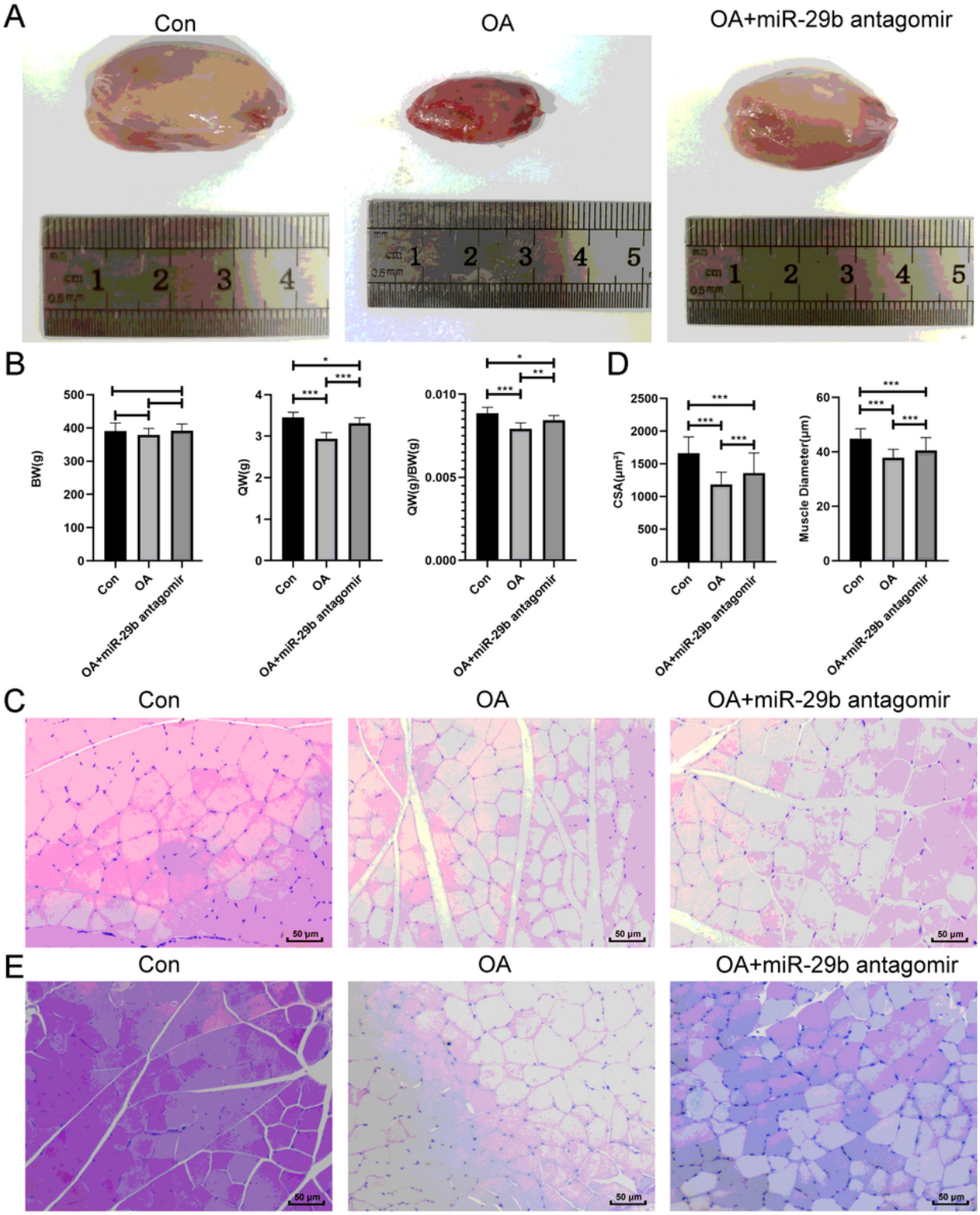

Figure 2

Weight-bearing ability and morphology of the quadriceps muscle in the rat model of KOA. (A) A typical picture of the quadriceps muscle of each group. (B) Body weight, quadriceps weight, and quadriceps weight/body weight ratio. (C) Hematoxylin–eosin staining of the quadriceps muscle. (D) The diameter and cross-sectional area of the quadriceps. (E) Periodic acid–Schiff staining of the quadriceps. Scale bar = 50 μm. *P < 0.05, **P < 0.01, and ***P < 0.001.

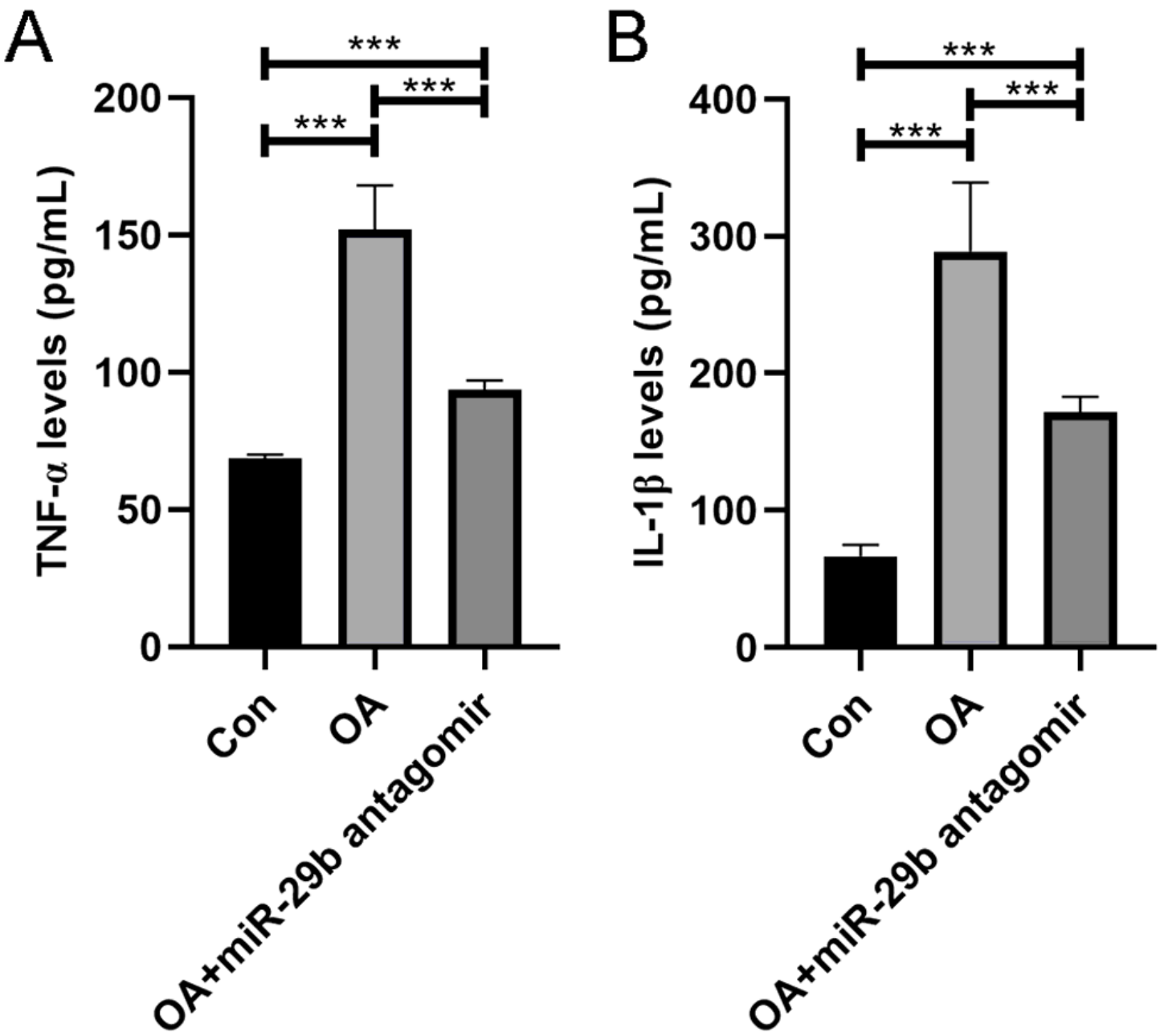

Figure 3

Levels of inflammatory cytokines in rat sera. (A) Expression of TNF-α. (B) Expression of IL-1β. *P < 0.05, **P < 0.01, and ***P < 0.001.

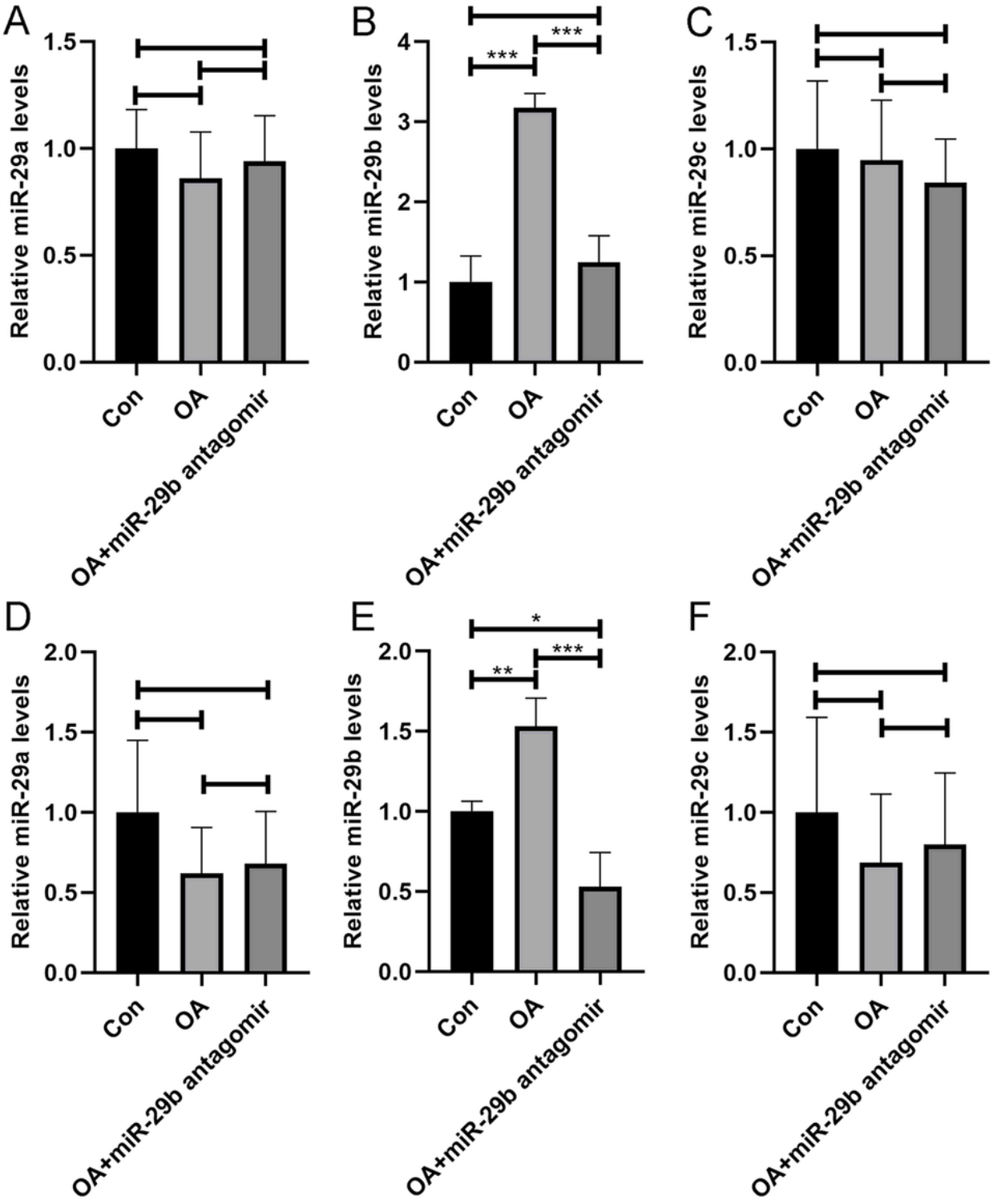

Figure 4

Levels of microRNAs in the miR-29 family in the joint and quadriceps muscle. (A) Expression of miR-29a in the joint. (B) Expression of miR-29b in the joint. (C) Expression of miR-29c in the joint. (D) Expression of miR-29a in the quadriceps muscle. (E) Expression of miR-29b in the quadriceps muscle. (F) Expression of miR-29c in the quadriceps muscle. *P < 0.05, **P < 0.01, and ***P < 0.001.

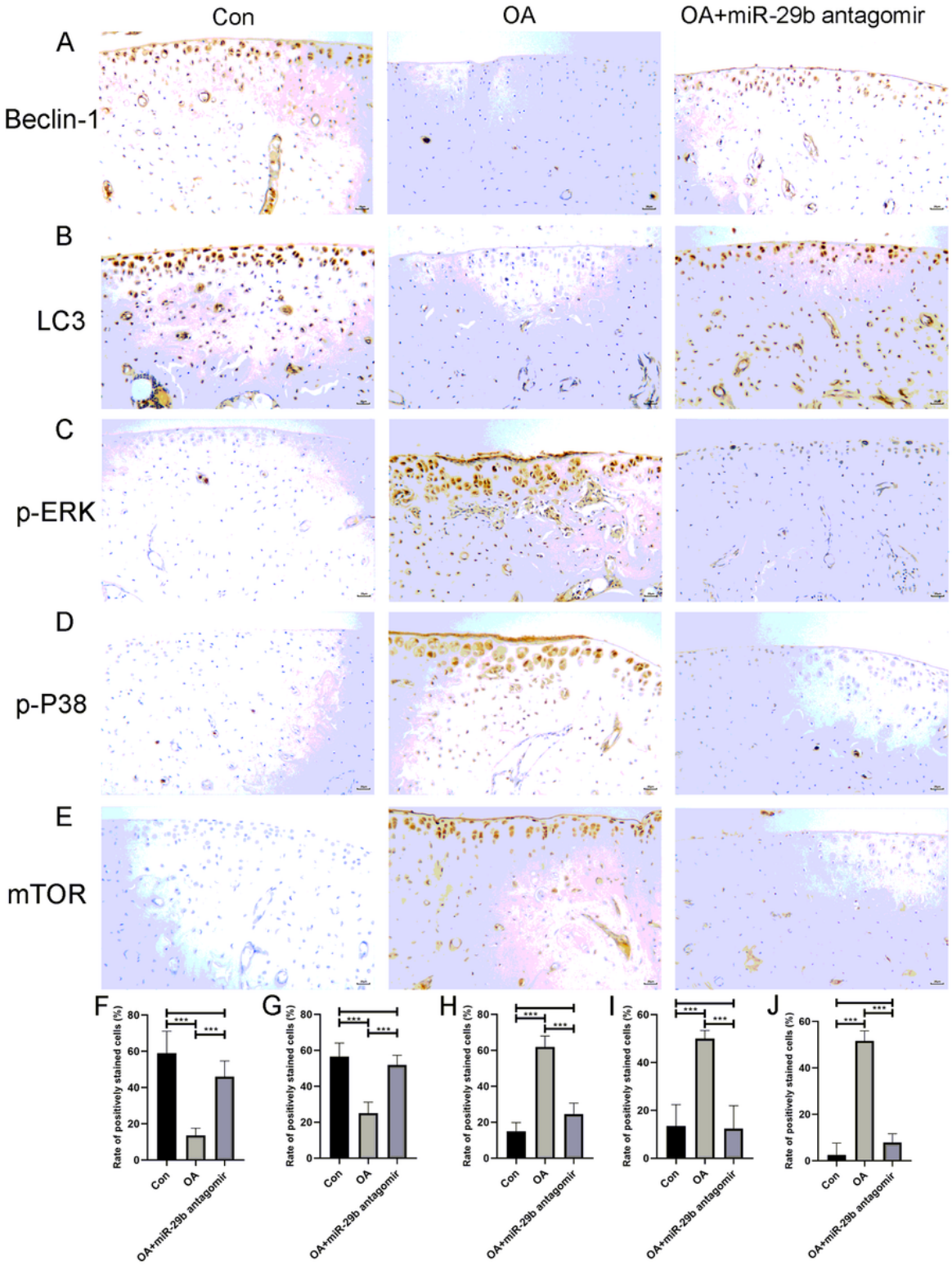

Figure 5

Immunohistochemistry for the expression of autophagy-related proteins in the cartilage of rats with KOA. (A) Expression of beclin-1. (B) Expression of LC3. (C) Expression of p-ERK. (D) Expression of p-P38. (E) Expression of mTOR. (F)–(J) Quantitative analysis of protein expression. *P < 0.05, **P < 0.01, and ***P < 0.001.

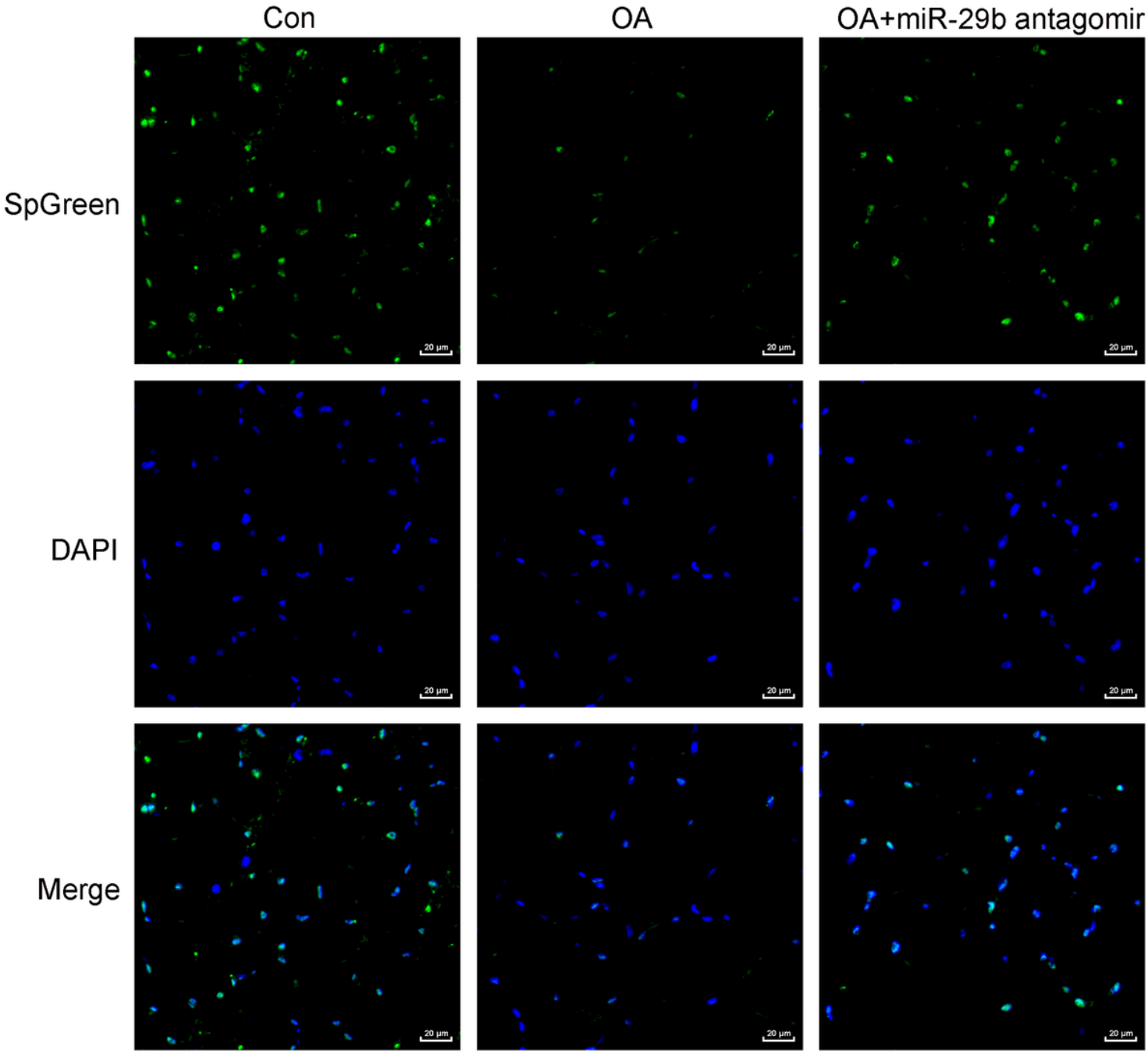

Figure 6

Immunofluorescence for the expression of the atrophy-related protein PI3K in the rat quadriceps muscle.

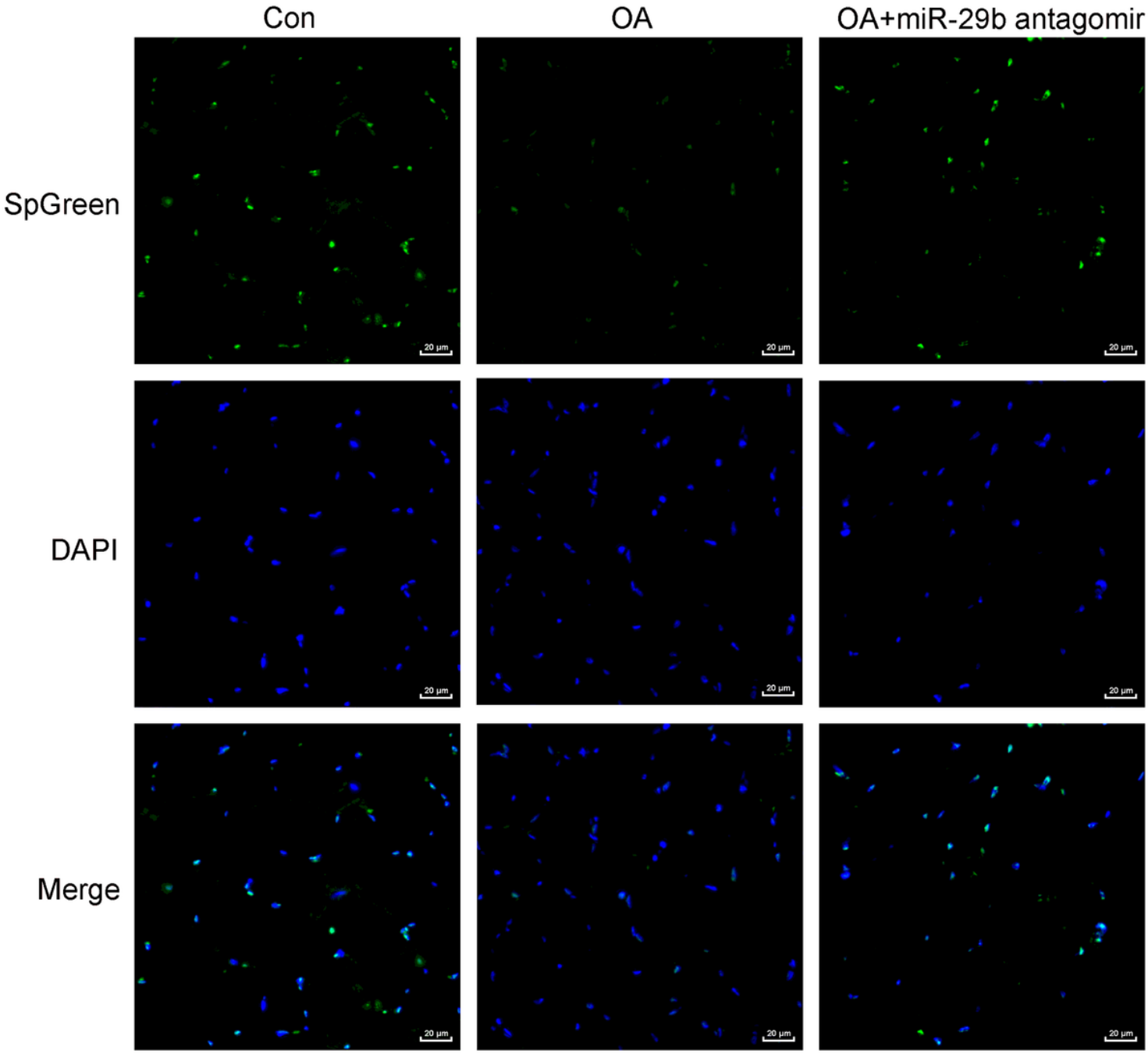

Figure 7

Immunofluorescence for the expression of the atrophy-related protein p-AKT in the rat quadriceps muscle.

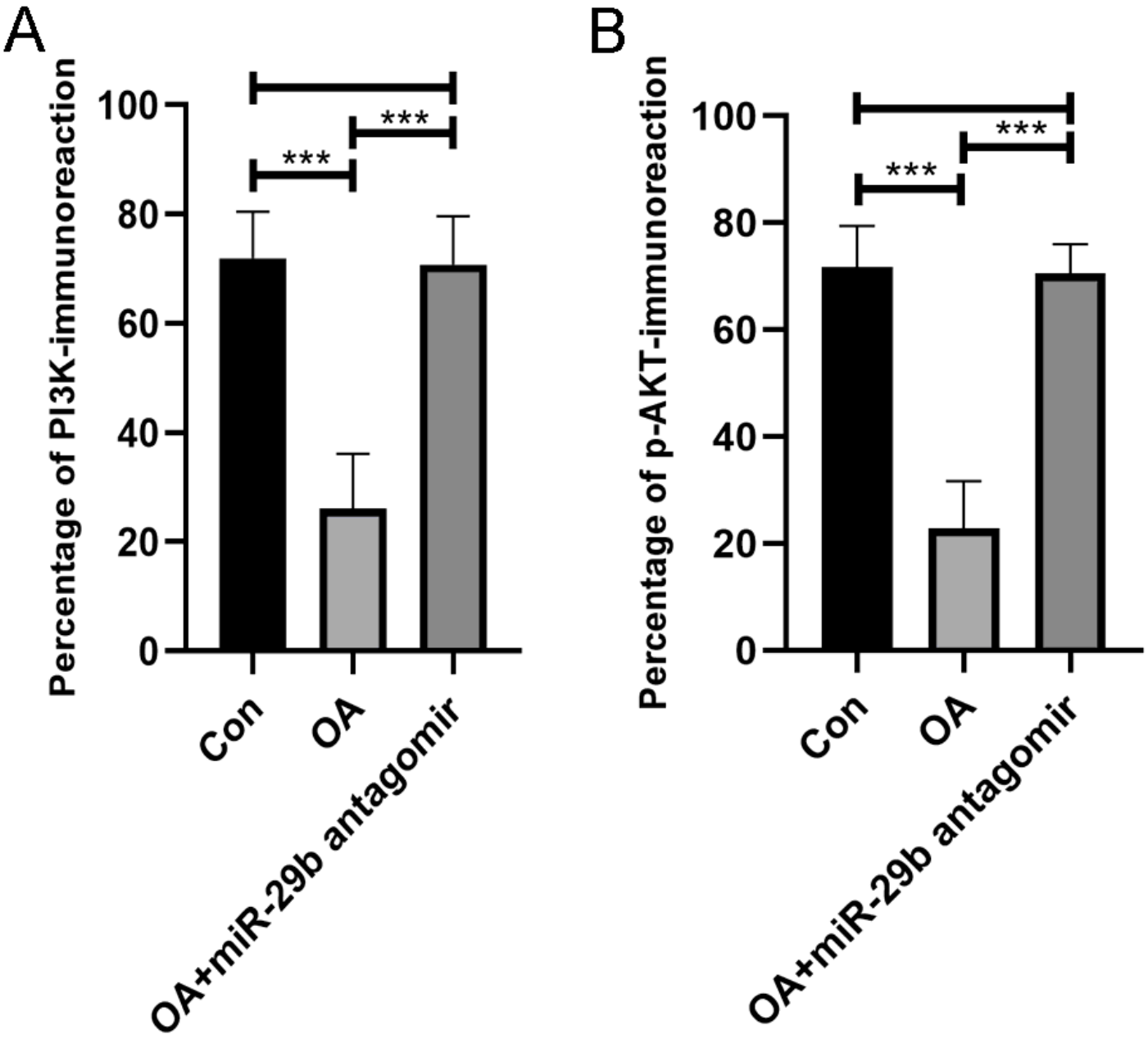

Figure 8

Quantitative analysis of PI3K and p-AKT expression. *P < 0.05, **P < 0.01, and ***P < 0.001.

Supplementary Files

This is a list of supplementary files associated with this preprint. Click to download.

- AuthorChecklistE10only.pdf